PHYSICAL REVIEW D VOLUME 40, NUMBER 7 1 OCTOBER 1989

Weak decays of K and π mesons

H. Galić
Stanford Linear Accelerator Center, Stanford University, Stanford, California 94309
(Received 23 December 1988)

Through a special interplay of strong and weak interactions, small but significant pieces with "wrong" flavor could be introduced into wave functions of mesons. Thus, e.g., not only a $(u\bar{s})$ pair, but also a $(u\bar{d})$ pair can be found with some probability within K^+, etc. The possible importance of such "anomalous" terms in understanding of K-meson decays is discussed in a new scheme. The scheme is characterized by diagrammatic calculations of full amplitudes in the long-distance environment. Two classes of models which correctly reproduce the main K-meson branching ratios and the $\Delta I=1/2$ rule are constructed. The predictive power of the scheme is then tested in a decay of a kaon into a pion and a light hyperphoton.

I. INTRODUCTION

The amplitude A^+_{+0} for $K^+\to\pi^+\pi^0$ decay is about 20 times smaller than amplitudes for two similar K_S decay modes. Yet, almost any simple theoretical consideration would put these three amplitudes into the same range. It becomes even more obvious how small A^+_{+0} is when a comparison to CP-violating $K_L\to\pi\pi$ decays is done. Despite the fact that CP-violating phenomena are extremely rare, there is only another factor-20 difference between A^+_{+0} and A^L_{+-} (A^L_{00}). Thus the A^+_{0+} amplitude lies just in the middle between CP-conserving and CP-violating amplitudes. What causes such a suppression of $K^+\to\pi^+\pi^0$? Is the decay really suppressed, or are—on the contrary—the decay modes of short- and long-lived neutral kaons largely enhanced? One possible solution was suggested in 1960, by Oneda, Pati, and Sakita.[1] They realized that a direct transformation of the constituent carrying the strangeness can be the key factor in description of experimental facts. Such a transformation, if it happened at a relatively high rate, would enhance $\Delta I=\frac{1}{2}$ decay amplitudes of neutral kaons, while not affecting $K^+\to\pi^+\pi^0$ decay. (See also Ref. 2.) This idea is still very much alive. There are many indications that a fast, flavor-changing $s\to d$ transition within a single quark line is indeed the major candidate for a natural explanation of both the $\Delta I=\frac{1}{2}$ rule and the large CP violation in the kaon multiplet. However, the detailed mechanism is still not well understood.[3,4]

One popular representation of these direct transitions was based on "penguin" operators and diagrams, incorporated into the QCD-corrected effective Hamiltonian.[5] Nowadays, as we learn more about the role of long-distance QCD in kaon decays, the $s\to d$ transitions reappear in the "eye diagrams"[6,7] which are in a way a link between short and long distances. In the present work, the $s\to d$ transitions are once again used to describe $K\to\pi\pi$ amplitudes, this time, however, set entirely in the long-distance environment.

I will present a scheme in which a diagrammatic calculation of K (and π) decays is possible. Quark loops in diagrams are closed by nonlocal meson-quark vertices mimicking meson wave functions. In addition to "regular" vertices, the model also contains "anomalous" meson-quark vertices, with unusual flavor content. The latter are a result of $s\to d$ transitions happening *inside* the light mesons. One therefore finds not only a $(u\bar{s})$ pair, but also a $(u\bar{d})$ pair within K^+, etc. "Regular" and "anomalous" vertices will be constructed and discussed in Sec. II. Rules for evaluation of diagrams and amplitudes will be given in Sec. III. Sections IV and V contain a brief review of the most important results. (More detailed study of the main K decay modes is presented elsewhere.)[8,9] In the concluding section the features of the model are summarized, and some possible directions for further study indicated. A different representation of anomalous vertices ("model B") is described in the Appendix.

Throughout the work the four-flavor version of the standard model is used, but a generalization to more flavors presents no problem. The notation closely follows that of an earlier work[8] on the subject. (See also Refs. 9–11.)

II. MODEL

In this section the attention will be focused on the relationship between light mesons and their constituents. The final goal will be a construction of semiphenomenological meson-quark couplings, which will serve later in diagrammatic calculations of various processes. A diagrammatic approach to K decays was attempted earlier by Pascual and Tarrach.[12] There are however differences between Ref. 12 and the present work. For example, only local meson-quark vertices were used in Ref. 12, while here the vertices will be nonlocal. More recently, Gilmour[13] has also presented a diagrammatic study of hadronic weak decays, but in a nonrelativistic framework. Here, I will develop a fully relativistic picture.

Let $H(k,P)$ be a probability for finding a combination of quarks with relative momentum $q_1-q_2=2k$, within a meson carrying the total momentum P (see Fig. 1). Such a probability distribution would clearly be related to the

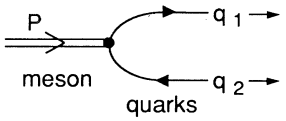

FIG. 1. Quark content of a meson in the valence approximation. The momentum of the antiquark is $q_2=P-q_1$.

wave function of the meson, and vice versa. Unfortunately, we do not know too much about meson wave functions. Yet, by using some acceptable assumptions, one can try to *model* the distributions $H(k,P)$, and then to test them in analyses of decay and scattering processes.

I will begin with the assumption that the distribution $H_{\mathcal{M}}(k,P)$ for the meson $\mathcal{M}$ is proportional to $1/(k^2-\alpha_{\mathcal{M}}P^2)^n$. The parameter $\alpha_{\mathcal{M}}$ has the value related to the weak decay constant $f_{\mathcal{M}}$ of the particular meson. For all the mesons considered in this study, the relation $\alpha_{\mathcal{M}}>\frac{1}{4}$ is satisfied. The integer n is a free parameter. There are some physical arguments for the above choice of $H_{\mathcal{M}}$. For example, according to the proposed form, the situations less likely to occur are those in which the relative (three-)momentum $\mathbf{k}$ is large, or when the energy is consumed mainly by one of the quarks. An asymmetry introduced by adding a $k\cdot P$ piece into the denominator of $H_{\mathcal{M}}$ would probably improve the agreement with experiments, but for sake of simplicity I will not allow the asymmetric terms. Needless to say, the presented form of $H_{\mathcal{M}}$ is by no means unique, and readers are encouraged to find and test different functional forms.

Once the proper Lorentz structure for pseudoscalar mesons is added, the normalized probability distribution becomes a matrix:

$$H_{\mathcal{M}}(k,P)=\beta_{\mathcal{M}}M_{\mathcal{M}}^{2n-3}\frac{\not{P}\gamma_5}{(k^2-\alpha_{\mathcal{M}}P^2)^n}\ , \tag{1}$$

where β is a dimensionless normalization constant, and M is the mass of the meson $\mathcal{M}$ (more on β in Ref. 8). One can also introduce a naive confinement into the model. This is most easily accomplished by sandwiching $H_{\mathcal{M}}$ between $(\not{k}+\not{P}/2-m_1)$ and $(\not{k}-\not{P}/2-m_2)$, where m_1 and m_2 denote the current masses of the quarks attached to the meson. Then, it is the equation of motion that prevents the unwanted decay to free quarks. The resulting nonlocal vertex[8]

$$\Gamma^{ij}_{\mathcal{M}}(k,P)=\delta^{ij}\left[\not{k}+\frac{\not{P}}{2}-m_1\right]H_{\mathcal{M}}(k,P)\left[\not{k}-\frac{\not{P}}{2}-m_2\right] \tag{2}$$

will be used in a diagrammatic description of mesons, and weak processes in which the mesons participate. The vertex (2) is named the "regular vertex." The symbol for a regular vertex in a diagram will be a heavy dot. Superscripts i,j in (2) denote colors, and δ^{ij} reflects the color conservation. The vertex implicitly contains all the interactions responsible for keeping quarks within the meson, and gluons hidden in the vertex are responsible for the nonlocal structure. The situation is symbolically described in Fig. 2.

How and where can one use the effective vertices? Consider $\pi^+\to\bar{l}\nu$ decay. To obtain the nonleptonic part of the amplitude (see Fig. 3), we should first multiply the probability of finding u and $\bar{d}$ quarks with relative momentum $2k$, by the probability that these quarks meet and form a W meson. Next, contributions of all possible relative momenta must be summed up. As a consequence, the amplitude contains an integral

$$\int d^4k\ \mathrm{Tr}\left[\gamma_\mu(1-\gamma_5)\frac{i}{\not{k}+\not{P}/2-m_u}\times\Gamma^{ij}_{\pi}(k,P)\frac{i}{\not{k}-\not{P}/2-m_d}\right]. \tag{3}$$

Note that Feynman propagators of u and d quarks will cancel similar factors in Γ. After the cancellation, the integral in (3) can be easily evaluated, and a straightforward calculation leads to the amplitude. More examples can be found in Refs. 8 and 9, where regular vertices were thoroughly studied.

Until now, the flavor of quarks was mostly ignored. It was implicitly assumed that, e.g., in the case of the K^+ meson, one would find u quark and s antiquark, with probability equal to 1. However, weak interactions can change the situation. Consider the diagram in Fig. 4. If the W boson is captured by the same quark line by which it was emitted, one would observe $\bar{d}$ instead of $\bar{s}$. What is the probability for such a flavor-changing transformation within a line? Without the gluons, for bare quarks, the process is down by $1/M_W^4$, and thus practically unobservable. Miraculously, gluons (and this is true for both "self-energy" gluons, and those exchanged between two different quark lines) acts as catalysts. It is known[5,14,15] that in their presence the probability for $s\to d$ transition gets increased to the much more comfortable $1/M_W^2$. Therefore, the probability distribution $\tilde{H}(k,P)$ for finding a quark with the "wrong" flavor in a meson, is of the order $G_F sc$, where s and c denote the Cabibbo angles ($s\equiv\sin\theta_C$, $c\equiv\cos\theta_C$). In many processes this will still be invisible, but in certain situations even such a small contribution might become very important. For example, the probability of forming a $\bar{d}d$ pair in K_S is small, but once the pair is formed, the meson can decay very quickly through a fast, flavor-conserving process. Thus the smallness of $\tilde{H}$ could be in some cases counterbalanced by an increased likelihood of the subsequent stronglike subprocess.

Of course, the functional form of $\tilde{H}(k,P)$ can only be guessed. In order to keep the analysis as simple as possible, I will again assume the probability distribution in the form of an inverse power of $(k^2-\alpha P^2)$. Guided by some

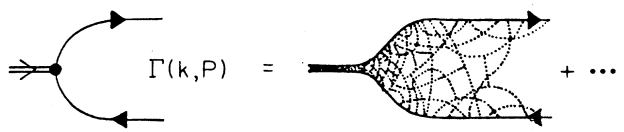

FIG. 2. Nonlocal, effective coupling of quarks to a meson.

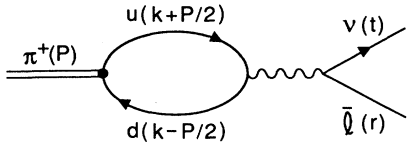

FIG. 3. $\pi^+ \to \bar{l}\nu$ decay. P is the momentum of the pion, k the loop momentum.

one-loop arguments, I am proposing the following expressions for the distribution $\tilde{H}$, and the "anomalous" (so named because of the presence of the "wrong" flavor) vertex function $\tilde{\Gamma}$:

$$\tilde{H}_{\mathcal{M}}(k,P)=\frac{G_F sc}{\sqrt{2}}\beta_{\mathcal{M}}M_{\mathcal{M}}^{2n-1}\mathcal{Q}^2\frac{\not{P}(X+Y\gamma_5)}{(k^2-\alpha_{\mathcal{M}}P^2)^{n+1}}\ , \tag{4}$$

$$\tilde{\Gamma}^{ij}_{\mathcal{M}}(k,P)=\delta^{ij}\left[\not{k}+\frac{\not{P}}{2}-m'\right]\tilde{H}_{\mathcal{M}}(k,P)\left[\not{k}-\frac{\not{P}}{2}-m''\right]\ . \tag{5}$$

Here, $\mathcal{Q}^2$ denotes the square of the momentum in the line in which the $s\to d$ transition occurs ($\mathcal{Q}$ is either $k-P/2$ or $k+P/2$). α and β are the parameters already defined in "regular" functions (1) and (2). The numerator in $\tilde{H}(k,P)$ contains the $(X+Y\gamma_5)$ matrix with mixed chirality. This is a consequence of the violation of parity in the weak transition. The model does not predict magnitudes of X and Y. They are parameters to be determined experimentally. I will, however, assume that X and Y do not depend on $\mathcal{M}$. It is interesting that in some processes only X contributes (e.g., in $K\to\pi\pi$), while in other decays Y is important (e.g., in $K\to\pi+\gamma_Y$, where γ_Y denotes a hyperphoton), or a combination of both appears (e.g., in $K\to\pi\bar{\nu}\nu$). As a consequence, it will be impossible to relate $K\to\pi\pi$ and $K\to\pi\gamma_Y$ decays directly, without introducing further assumptions. We shall return to this problem in Sec. V. The anomalous vertices will be denoted in diagrams by encircled heavy dots.

Not only that the flavor and chiral structure of the anomalous vertices is unusual, there is also a peculiarity related to isospin. Since in a direct $s\to d$ transition the isospin is changed by only $\frac{1}{2}$ unit, the anomalous vertices cannot contribute to $\Delta I=\frac{3}{2}$ processes.[1] In other words, in the analysis of, e.g., $K^+\to\pi^+\pi^0$ (which is a pure $\Delta I=\frac{3}{2}$ decay), all diagrams with anomalous vertices should exactly cancel. This clearly provides a mechanism for a successful description of the $\Delta I=\frac{1}{2}$ rule. Namely, the hadronic $K^\pm$ decays will only be influenced by regular vertices. As a rule, the regular vertices produce small amplitudes. On the other hand, the amplitudes A^S will mainly depend on the magnitude of X. Large X would produce big A^S without increasing the $A^\pm$ amplitudes. Consequently, since X is a free parameter, the ratio $A^S/A^\pm$ can easily be adjusted to the required value of 20.

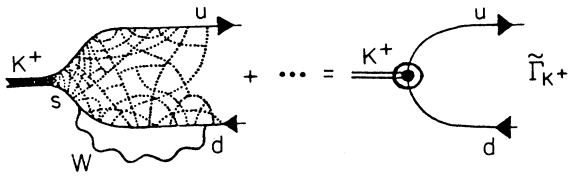

FIG. 4. Substructure of an "anomalous" vertex.

Finally, in order to get some control over the model dependence, I have constructed another anomalous probability distribution. It is presented in the Appendix. The expressions (4) and (5) in this section will be referred to as "model A," and the alternative model from the Appendix will be called "model B."

III. RULES

In this section we shall consider how the effective vertices can be put to work in a diagrammatic calculation of light-meson decays. First, one must construct all possible (lowest-order) Feynman diagrams of a process, using quark, lepton, and electroweak-boson lines. Gluons, according to the scheme, should be neglected. Instead, the regular and anomalous quark-meson vertices should be used to close quark lines. Mesons are always on shell, external particles, and cannot be used as intermediate states. In closed fermion loops, a summation over Fermi and color degrees of freedom must be performed. Accordingly, a trace calculation and the factor (-3) will accompany every quark loop (the negative sign in the factor is a consequence of the Fermi statistics). Elementary particles (quarks, leptons,. . .) and pointlike electroweak interactions are represented by the usual Feynman propagators and vertices. The nonlocal effective vertices, both regular and anomalous, should be described following the general rules derived in the preceding section. However, a distinction between mesons forming an isotriplet, isodoublet, or isosinglet should be visible in the effective vertices. Therefore, each probability function $H_{\mathcal{M}}(k,P)$ will be multiplied by a Clebsch-Gordan (CG) coefficient λ. Instead of (2), one uses

$$\Gamma^{ij}_{\mathcal{M}}(k,\pm P)=\pm\lambda\delta^{ij}\left[\not{k}\pm\frac{\not{P}}{2}-m_q\right]H_{\mathcal{M}}(k,P)\times\left[\not{k}\mp\frac{\not{P}}{2}-m_{q'}\right]\ . \tag{6}$$

$\Gamma(k,+P)$ should be used when the meson is ingoing, and $\Gamma(k,-P)$ when it is outgoing. The values of λ are $+1$ for $K^\pm,\pi^\pm$ vertices, $+1/\sqrt{2}$ for $\pi^0(\bar{u}u)$, $K_L(\bar{d}s)$, $K_L(\bar{s}d)$, and $K_S(\bar{d}s)$ vertices, $-1/\sqrt{2}$ for $\pi^0(\bar{d}d)$ and $K_S(\bar{s}d)$ vertices, etc. Constants $\alpha_\pi,\alpha_K,\ldots,$ in $H_{\mathcal{M}}$ could be related to values of weak decay constants $f_\pi,f_K,\ldots,$ while $\beta_\pi,\beta_K,\ldots,$ properly normalize the wave functions. One finds[8]

$$\alpha_{\mathcal{M}}=\pi\frac{f_{\mathcal{M}}}{M_{\mathcal{M}}}\left[\frac{(n-1)(n-2)^2}{6(2n-1)}\right]^{1/2},\qquad \beta_{\mathcal{M}}=4\pi\alpha_{\mathcal{M}}^{n-1}\left[\frac{(2n-1)(2n-2)}{3}\right]^{1/2}. \tag{7}$$

As discussed earlier, the anomalous vertices are a result of $s \to d$ (or $d \to s$) weak transitions within a meson. Therefore, in an anomalous vertex, a d quark will be attached where an s quark appears in the corresponding regular vertex, and vice versa: an s quark instead of the regular d quark (see Fig. 5). Where the flavor structure of regular vertices was, e.g., $K^+(\bar{s}u)$ and $\pi^0(\bar{d}d)$, the anomalous structure will be $K^+(\bar{d}u)$, $\pi^0(\bar{s}d)$, and $\pi^0(\bar{d}s)$, etc. The complete anomalous vertex function, instead of (5), becomes

$$\tilde{\Gamma}^{ij}_{\mathcal{M}}(k,\pm P)=\pm\lambda\delta^{ij}\left[\not{k}\pm\frac{\not{P}}{2}-m\right]\tilde{H}_{\mathcal{M}}(k,P) \times\left[\not{k}\mp\frac{\not{P}}{2}-m'\right]. \tag{8}$$

Again, $\tilde{\Gamma}(k,+P)$ describes an ingoing meson and $\Gamma(k,-P)$ an outgoing meson. The convention for CG coefficients λ is the same as in the corresponding regular vertices. The probability distribution $\tilde{H}_{\mathcal{M}}$ [see Eq. (4)] contains the square of momentum of the quark line in which the flavor is changed. In π^0, K^L, and K^S such a transmutation can happen in both quark lines. Therefore, e.g., the full anomalous vertex $K_S(\bar{d}d)$ contains a factor (compare to Fig. 6)

$$\lambda\tilde{H}_S\sim\frac{1}{\sqrt{2}}\left[k+\frac{P}{2}\right]^2-\frac{1}{\sqrt{2}}\left[k-\frac{P}{2}\right]^2. \tag{9}$$

The first term originates from the $s \to d$ transition in the upper line of the regular $K_S(\bar{d}s)$ vertex, and the second term is related to $\bar{s} \to \bar{d}$ transition in the lower quark line

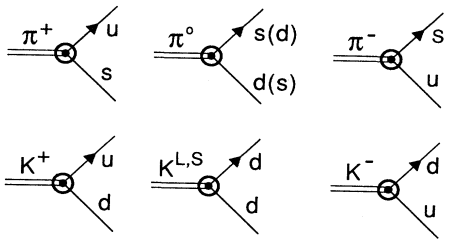

FIG. 5. Anomalous vertices for light in-going mesons.

of $K_S(\bar{s}d)$ (Fig. 6). Factors $\pm 1/\sqrt{2}$ are the CG coefficients. [For the $K_L(\bar{d}d)$ vertex, both terms in the analogous expression would be positive, because CG coefficients are different.]

We can now return to the example mentioned in Sec. II: namely, the $\pi^+ \to \bar{l}\nu$ decay (Fig. 3). Following the rules, one can express the amplitude of the process in terms of an integral which can be easily calculated (see Ref. 8). With the definition (7) for $\alpha_{\mathcal{M}}$ and $\beta_{\mathcal{M}}$, one obtains the familiar form (note: $g^2/8M_W^2=G_F/\sqrt{2}$)

$$A_{\text{reg}}=(-)^{n+1}\frac{G_F c}{\sqrt{2}}f_\pi\bar{u}_\nu(t)\not{P}(1+\gamma_5)v_l(r). \tag{10}$$

This is no surprise, since the relation (7) between $\alpha_{\mathcal{M}}$ and $f_{\mathcal{M}}$ was determined just in a study of $\mathcal{M}_{l2}$ decays. Also contributing to the process is a diagram (Fig. 7) with an anomalous vertex, but this diagram is very suppressed. The hadronic part of the amplitude A_{anom} (Fig. 7) is

$$(-3)i^2\int\frac{d^4k}{(2\pi)^4}\text{Tr}\left\{s\gamma_\mu(1-\gamma_5)\left[\frac{G_F sc}{\sqrt{2}}\beta_\pi M_\pi^{2n-1}\left[k-\frac{P}{2}\right]^2\frac{\not{P}(X+Y\gamma_5)}{(k^2-\alpha_\pi P^2)^{n+1}}\right]\right\} =(-)^n icf_\pi P^\mu\left[\frac{G_F s^2}{\sqrt{2}}M_\pi^2(X+Y)\left[\frac{2}{n}-\frac{n-2}{4n\alpha_\pi}\right]\right]. \tag{11}$$

Note that the hadronic part of the similar regular amplitude (Fig. 3) is exactly $(-)^n icf_\pi P^\mu$. Since $G_F M_\pi^2\sim 10^{-7}$, $s^2\equiv\sin^2\theta_C\sim 10^{-2}$, and $(X+Y)$ is ~ 1 (see the next section), the anomalous contribution is many orders of magnitude smaller than the regular one. Consequently, the anomalous diagram can be ignored safely in this decay. In the similar K_{l2} decay, the ratio $A_{\text{anom}}/A_{\text{reg}}$ is slightly larger ($\sim 10^{-6}$), but still negligible. In some other decays the situation will be identical: because of a hidden $s \to d$ transition, the anomalous vertex adds a second weak interaction, and the related anomalous amplitude becomes much smaller than the first-order (in weak interactions) regular amplitudes. However, we shall see in the next example that sometimes the suppression is absent, and then the diagrams with anomalous vertices become not only important, but also dominant, overshadowing all other

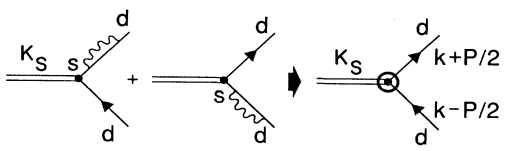

FIG. 6. Substructure of the anomalous $K_S(\bar{d}d)$ vertex.

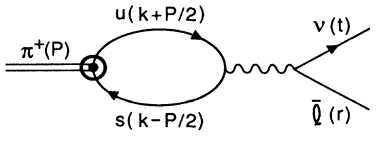

FIG. 7. The anomalous contribution to $\pi^+ \to \bar{l}\nu$ decay.

contributions.

Consider $K\to\pi\pi$ decays. We already know that diagrams with anomalous vertices should not contribute to $\Delta I=\frac{3}{2}$ decays. Indeed, it is easy to demonstrate an exact cancellation of anomalous diagrams in $K^+\to\pi^+\pi^0$. A^+_{+0} therefore receives a nonvanishing contribution $A^+_{\rm reg}$ from the regular diagrams only. A characteristic diagram is presented in Fig. 8. The decay is Cabibbo suppressed, and of the first order in weak interactions. The total amplitude can be written as[8]

$$A^+_{+0}=A^+_{\rm reg}\simeq\frac{G_F sc}{\sqrt{2}}M_K^2 f_\pi I\ , \tag{12}$$

where $I\sim\frac{1}{2}$ is a number whose exact value[16] depends on the parameter n in (1). In Ref. 8 it was also shown that the regular contributions to the decay of K_S are of the same order, since the diagrams are very similar: $(A^S_{+-})_{\rm reg}\sim(A^S_{00})_{\rm reg}\sim A^+_{\rm reg}$. This certainly cannot describe the experimental results: we know that A^S amplitudes should be much bigger. The diagrams with anomalous vertices will make a difference this time. Consider diagrams for $K_S\to\pi^+\pi^-$ sketched in Fig. 9 (a similar set can be constructed for $K_S\to\pi^0\pi^0$). The anomalous contributions in π_{l2} decay were negligible. On the contrary, by analyzing Fig. 9, one finds no suppression. Although the encircled vertices are of the order G_F, they also change the flavor structure in such a way that no further weak interaction is needed to complete the decay. Consequently, the diagrams with anomalous contributions (Fig. 9), and the regular diagram (Fig. 8), are at least of the same order. Moreover, parameters X and Y can help to inflate the anomalous amplitude even further, making it dominant. Let me illustrate this by analyzing the first diagram in Fig. 9.

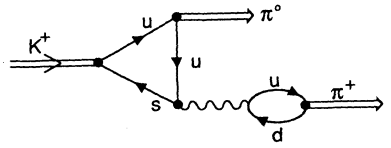

FIG. 8. A typical regular contribution to $K\to\pi\pi$. Other regular diagrams are analyzed in Ref. 8.

According to the rules, the amplitudes can be written after some rearrangement as

$$\tilde{A}(1)=\frac{G_F sc}{\sqrt{2}}(\beta_K M_K^{2n-1})(\beta_\pi M_\pi^{2n-3})^2(-3)i^3$$
$$\times\int\frac{d^4k}{(2\pi)^4}\frac{1}{\sqrt{2}}\left[\left[k+\frac{P}{2}\right]^2-\left[k-\frac{P}{2}\right]^2\right]\mathrm{Tr}\left[\left[\not k+\frac{\not P}{2}-m_d\right]\frac{\not P(X+Y\gamma_5)}{B^{n+1}}\right.$$
$$\left.\times\left[\not k-\frac{\not P}{2}-m_d\right]\frac{\not S\gamma_5}{C^n}\left[\not k+\frac{\not S-\not R}{2}-m_u\right]\frac{\not R\gamma_5}{D^n}\right]\ . \tag{13}$$

Here, the denominators are

$$B=k^2-\alpha_K P^2,\quad C=(k-R/2)^2-\alpha_\pi S^2\ ,$$
$$D=(k+S/2)^2-\alpha_\pi R^2\ , \tag{14}$$

and P,R,S are momenta of K_S,π^-,π^+ respectively. It is easy to see that the $Y\gamma_5$ term from the anomalous vertex does not contribute. Indeed, traces of all terms proportional to Y vanish. The analytic calculation with expressions similar to (13) is impractical, but after the evaluation of traces, one can calculate the remaining (convergent) integrals numerically. In our particular case, the amplitude finally gets the form

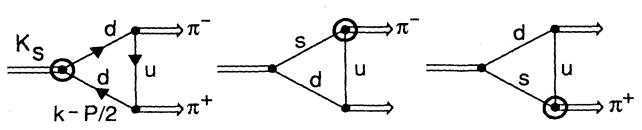

FIG. 9. Anomalous vertices in $K_S\to\pi^+\pi^-$ decay.

$$\tilde{A}(1)=\frac{G_F sc}{\sqrt{2}}M_K^2 f_\pi X\tilde{I}(1)\ . \tag{15}$$

(The tilde in this paper will always be used to denote the anomalous contributions.) X is the parameter from the anomalous vertex, and $\tilde{I}(1)$ a number which sharply depends on the model parameter n. For $n=5$, one finds $|\tilde{I}(1)|\approx 8$, and the ratio of the typical regular [Eq. (12)] and anomalous amplitudes becomes

$$[\tilde{A}(1)/A^+_{\rm reg}]_{n=5}\sim[\tilde{I}(1)/I]_{n=5}X\sim 15X\ . \tag{16}$$

Let A^S_{+-} denote the total (regular+anomalous) amplitude. The famous ratio A^S_{+-}/A^+ can now be expressed in terms of X. From (16) it follows that if the model adopts a value of X of the order of 1, the successful parametrization of the $\Delta I=\frac{1}{2}$ dominance is achieved. (For a different parameter n, a different value of X will do the job.) The complete result, which also includes contributions of the remaining two diagrams in Fig. 9, will be displayed in the next section. Once the n is chosen and the constant X is fixed, the model gains a predictive power, which should be used in analyses of other processes. We shall further study $K\to\pi\pi$ and some other K decays in Secs. IV and V.

IV. DETAILED STUDY OF MAIN DECAY MODES OF KAONS

In the previous section some general features of the model were briefly illustrated. This section is devoted to a more detailed analysis of the main decay modes of K mesons. Parameters of both regular and anomalous vertices are fixed, and the theoretical results are compared to experiments. Finally, in the next section, the predictive power of the theory will be tested in an interesting rare decay.

We shall not spend too much time considering processes in which the important contribution comes only from diagrams with regular vertices. The procedure is described in Ref. 8, and I will present only the final results here. The processes are listed in Table I. Within the scheme, it is possible to describe all these leptonic and semileptonic decays of K and π by adjusting only two parameters, α_π and α_K. The results in Table I are calculated with $n=5$, where n is the power in the denominators of vertex functions. Parameters α were determined by analyzing the $\pi^+\to\mu^+\nu$ and $K^+\to\mu^+\nu$ decays, and were found to be

$$\alpha_\pi^{(5)}=2.387, \quad \alpha_K^{(5)}=0.822 . \tag{17}$$

The index in parentheses stands for $n=5$. The above values correspond to $f_\pi=130$ MeV, $f_K=160$ MeV, $\beta_\pi=1998.6$, and $\beta_K=28.1$; see the expressions in Eq. (7). Once the α's are fixed, a straightforward procedure leads to the decay rates for other processes listed in Table I. A look at the table reveals a fair general agreement between theoretical and experimental numbers. For a complete discussion of these results, see Ref. 9.

Let us turn now to the study of decays of the neutral kaons. Though the regular vertices contribute to K_L and K_S decays, then cannot account for more than 15% of the total A_{00}^S or A_{+-}^S amplitudes. Indeed, it was shown in Ref. 8, that

$$(A_{00}^S)_{\rm reg}=+\tfrac{1}{2}A_{+0}^+, \quad (A_{+-}^S)_{\rm reg}=-\tfrac{3}{2}A_{+0}^+ ,$$
$$(A_{00}^L)_{\rm reg}=0, \quad (A_{+-}^L)_{\rm reg}=0 . \tag{18}$$

TABLE I. Theoretical (with parameter $n=5$) and experimental branching ratios for decays in which only diagrams with regular vertices contribute. The first two significant digits are displayed in the results.

Process	Theory	Experiment
$\pi^+\to\mu^+\nu$	Input[a]	100%
$\pi^+\to e^+\nu$	1.3×10^{-4}	1.2×10^{-4}
$\pi^+\to\pi^0e^+\nu$	1.0×10^{-8}	1.0×10^{-8}
$K^+\to\mu^+\nu$	Input[b]	0.64
$K^+\to e^+\nu$	1.6×10^{-5}	1.5×10^{-5}
$K^+\to\pi^0e^+\nu$	0.035	0.048
$K^+\to\pi^0\mu^+\nu$	0.023	0.032
$\Gamma(K_{e3}^+)/\Gamma(K_{\mu3}^+)$	0.66	0.66
$K_L\to\pi^-e^+\nu$ (or $\pi^+e^-\bar\nu$)	0.14	0.19
$K_L\to\pi^-\mu^+\nu$ (or $\pi^+\mu^-\bar\nu$)	0.10	0.14
$K_L\to K^-e^+\nu$ (or $K^+e^-\bar\nu$)	2.7×10^{-9}	N.A.
$\Gamma(K_{Le3})/\Gamma(K_{L\mu3})$	0.66	0.70
$K_S\to\pi^-e^+\nu$ (or $\pi^+e^-\bar\nu$)	2.5×10^{-4}	N.A.
$K_S\to\pi^-\mu^+\nu$ (or $\pi^+\mu^-\bar\nu$)	1.6×10^{-4}	N.A.
$K_S\to K^-e^+\nu$ (or $K^+e^-\bar\nu$)	4.7×10^{-12}	N.A.

[a]Input for α_π.
[b]Input for α_K.

[Note that the second line in (18) reflects the absence of CP violation in the four-flavor model.] Numerically, the $(A^S)_{\rm reg}$ amplitudes calculated with (12) and (18) are not bigger than 50 eV, while the experimental numbers are on the order of 400 eV. Therefore, from now on I will totally neglect the regular diagrams in the analysis of the $K_S\to\pi\pi$ decays, and concentrate only on diagrams with anomalous vertices. The first to be considered are the diagrams in which only one of the regular vertices is replaced by a vertex with an anomalous flavor structure. Such diagrams for $K_S\to\pi^+\pi^-$ decay are depicted in Fig. 9, and one of the amplitudes, $\tilde A(1)$, is displayed in Eq. (13). The remaining two amplitudes are

$$\tilde A(2)+\tilde A(3)=\frac{G_F sc}{\sqrt2}(\beta_K M_K^{2n-3})(\beta_\pi M_\pi^{2n-2})^2(-3)i^3$$
$$\times\int\frac{d^4k}{(2\pi)^4}\frac{1}{\sqrt2}\left\{\left[k+\frac{P}{2}\right]^2\mathrm{Tr}\left[\left[\not k+\frac{\not P}{2}-m_s\right]\frac{\not P\gamma_5}{B^n}\left[\not k-\frac{\not P}{2}-m_d\right]\frac{\not S\gamma_5}{C^n}\right.\right.$$
$$\left.\times\left[\not k+\frac{\not S-\not R}{2}-m_u\right]\frac{\not R(X+Y\gamma_5)}{D^{n+1}}\right]$$
$$-\left[k-\frac{P}{2}\right]^2\mathrm{Tr}\left[\left[\not k+\frac{\not P}{2}-m_d\right]\frac{\not P\gamma_5}{B^n}\left[\not k-\frac{\not P}{2}-m_s\right]\frac{\not S(X+Y\gamma_5)}{C^{n+1}}\right.$$
$$\left.\left.\times\left[\not k+\frac{\not S-\not R}{2}-m_u\right]\frac{\not R\gamma_5}{D^n}\right]\right\}. \tag{19}$$

The denominators B, C, and D were defined in Eq. (14). When contributions of all three diagrams are summed, the total *anomalous* amplitude can be written as

$$\tilde{A}^{S}_{+-}=\frac{G_F sc}{\sqrt{2}}M_K^2 f_\pi X \tilde{I} \ . \tag{20}$$

Here, $\tilde{I}$ denotes a sum of loop integrals, which must be calculated numerically. In model A, with $n=5$, one finds $\tilde{I}\to\tilde{I}^{A}_{(5)}=5.00$. (For the model B results, see the Appendix.) X in (20) is the unknown parameter, sitting in the anomalous vertex, see Eq. (4). One also easily finds that $\tilde{A}^{S}_{00}=\tilde{A}^{S}_{+-}$. The anomalous amplitudes in terms of the parameters X are given in Table II, for both model A and model B. If the anomalous vertices are responsible for the $\Delta I=\frac{1}{2}$ dominance, the free parameters must assume the values

$$\begin{aligned} X^{A}_{(5)}&\simeq 1.3 \quad \text{(model A)} \ , \\ X^{B}_{(5)}&\simeq -6.8 \quad \text{(model B)} \ . \end{aligned} \tag{21}$$

With these values, two $K_S\to\pi\pi$ amplitudes get the magnitude of about 376 eV. The remaining fine splitting between $(A^{S}_{00})_{\text{expt}}$ and $(A^{S}_{+-})_{\text{expt}}$ could be achieved if the small regular contributions (18) are added to the anomalous amplitudes with a certain phase angle.

It is important to note that in $K_S\to\pi\pi$ decays only the parameter X can be determined, but nothing can be said about the other parameter characterizing anomalous vertices: namely, Y [see Eq. (4)]. As a working hypothesis we can assume that this second parameter has a value not too different from X, and set $Y\approx X$. However, this is only a hypothesis, which still has to be confirmed (or rejected) in analyses of other decay channels.

What we have seen so far is that the diagrammatic calculation in the long-distance scheme can accommodate all the major decay modes of K (and π) to a good degree of accuracy, provided the parameter X has the proper value. What still remains is to test the model in rare decays. This will be done in the next section, in an analysis of an interesting, though not yet observed, decay mode of K^+.

TABLE II. Amplitudes (in eV) for $K\to\pi\pi$ decays. The anomalous contributions, calculated in models A and B (with $n=5$), are compared to experimental results. The latter were obtained from the measured decay rates (Ref. 36), by using $|A_{\text{expt}}|=(8\pi M_K^2\Gamma/|\mathbf{p}|)^{1/2}$. The statistical factor $\sqrt{2}$ is included in $(A^{S,L}_{00})_{\text{expt}}$.

Decay	Model A	Model B	Experiment
$K^+\to\pi^+\pi^0$	0	0	18
$K_S\to\pi^+\pi^-$	$285X^{A}_{(5)}$	$-55X^{B}_{(5)}$	389
$K_S\to\pi^0\pi^0$			372
$K_L\to\pi^+\pi^-$	0	0	0.9
$K_L\to\pi^0\pi^0$			0.8

V. K DECAYS AND FIFTH FORCE

Once we are convinced that some model successfully describes the basic K decays, we usually apply the model in a subsequent study of rare and/or unobserved kaon decays. This has repeatedly been done in the past, and will also be carried out in this work. Only such a procedure truly tests the predictive power of a scheme. Indeed, while a theoretical study of, e.g., $K\to\pi\pi$ decays is always in one way or another affected by the well-measured experimental numbers, the real nature of a model is revealed only when one is not in temptation of reproducing some of the firmly established data.

The decay channel which will be analyzed in this section is $K^+\to\pi^+\gamma_Y$. Here, γ_Y is the "hyperphoton"—an ultralight vector particle (with a mass possibly smaller than 10^{-8} eV) associated with the so-called fifth force.[17] This force might be responsible for effects observed in recent experiments measuring deviations from the ordinary gravity.[18–23] Note that the deviations in some of these experiments might also be a sign of a short-range quantum fluctuation in gravitational theory, and thus possibly unrelated to the fifth force. It would be much easier to distinguish between the two competing hypotheses if a clear effect is observed also in K decays. This is the main reason for renewed interest in $K^+\to\pi^+\gamma_Y$. Indeed, a better experimental limit and a reliable theoretical description of this decay could lead us to a firm confirmation of the fifth force, and give an important piece of information on its character and strength. Several excellent articles[24–27] about the new force were published recently, and the reader is referred to these reviews for further details. Presently, the experimental limit[28] on the branching ratio for $K^+\to\pi^+\gamma_Y$ decays is $B<4.6\times10^{-8}$. A new experiment[29] is expected to push this limit to the range 10^{-10} in the near future. The decay has also been studied by four groups of theorists.[30–33] An essential step in all the theoretical analyses was to relate matrix elements of $K\to\pi\gamma_Y$ to those of $K\to\pi\pi$ decays, and each group devised different methods to achieve that goal. Surprisingly, the quoted results for the branching ratio are spread over 2 orders of magnitude (see Table III). It will be interesting to see how our long-distance oriented model, with the direct evaluation of amplitudes, compares to other analyses.

The coupling of the hyperphoton to a quark can be described by the vertex $ifC_q\gamma^\tau$, where f denotes the general strength of the fifth force, and C_q is the hypercharge of the interacting quark. For example, $C_u=C_d=\frac{1}{3}$, $C_s=-\frac{2}{3}$, $C_c=\frac{4}{3}$, etc. In the nonrelativistic limit, the above form of the vertex corresponds to the Yukawa potential $V=(f^2/4\pi)\exp(-br)/r$. Note that Fischbach's group[25–27,31] uses a different Yukawa coupling, and their constant f^2 is 4π times smaller than the one used here. (This fact is important in the numerical comparison of various results, and has been taken into account in Table III.)

Two classes of diagrams have to be considered in an analysis of $K^+\to\pi^+\gamma_Y$ decay. In the first class, the diagrams are constructed without use of the anomalous vertices. A typical diagram is presented in Fig. 10. When

TABLE III. Various predictions for the branching ratio $B=\Gamma(K^+\to\pi^+\gamma_Y)/\Gamma(K^+)_{\rm all}$. All the results are given in terms of f^2 normalized according to the convention described in the text. Comments: (a) The common four-momentum in two-body matrix elements is taken to be the pion momentum; (b) with $r^2=1.5$ (r^2 is an enhancement factor due to a presence of the short-distance gluons); (c) with $r^2=12$; (d) corresponds to $x=0.29$ choice (x is a correction factor required because of an extrapolation to the zero-momentum poin); (e) model A, assuming $Y^A_{(5)}=X^A_{(5)}=1.3$; (f) model B, assuming $Y^B_{(5)}=X^B_{(5)}=-6.8$.

Ref.	B (in 10^{16} eV^2)	Comment
Aronson *et al.* (Ref. 31)	$0.5(f^2/m_Y^2)$	(a)
Suzuki (Ref. 30)	$4.4(f^2/m_Y^2)$	(b)
	$35.4(f^2/m_Y^2)$	(c)
Bouchiat *et al.* (Ref. 32)	$30.0(f^2/m_Y^2)$	(d)
Lusignoli *et al.* (Ref. 33)	$31.0(f^2/m_Y^2)$	
This work	$45.0(f^2/m_Y^2)$	(e)
	$2.5(f^2/m_Y^2)$	(f)

three similar diagrams are added, and the amplitude calculated with α's and β's as determined in (17), one finds

$$A^\tau_{\rm reg}=-i\frac{G_F sc}{\sqrt{2}}ff_\pi f_K(0.042)P^\tau+\cdots\ . \tag{22}$$

P^τ is the momentum of the kaon. The ellipsis denotes the part of the amplitude proportional to the hyperphoton momentum Q^τ. (This latter piece does not affect the decay rate.) Had (22) been the only contribution, the branching ratio would have been of the order $B\sim 2\times 10^{13}(f/m_Y)^2$ eV^2, which is much smaller than B obtained in the other analyses,[30–33] and beyond the present experimental limit. However, we know that the second class of diagrams, those with anomalous vertices, should also be considered. They are presented in Fig. 11.

In model A, after some rearrangement, the sum of the corresponding amplitudes can be written as

$$A^\tau_{\rm anom}=\frac{G_F sc}{\sqrt{2}}(\beta_K M_K^{2n-3})(\beta_\pi M_\pi^{2n-3})fY(-3)\times\int\frac{d^4k}{(2\pi)^4}\left[M_K^2\frac{C_u J^\tau(1)-C_d J^\tau(2)}{V^{n+1}U^n}+M_\pi^2\frac{C_u J^\tau(3)-C_s J^\tau(4)}{V^n U^{n+1}}\right], \tag{23}$$

where

$$V=k^2-\alpha_K M_K^2,\quad U=(k+Q/2)^2-\alpha_\pi M_\pi^2\ , \tag{24}$$

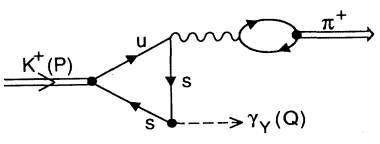

FIG. 10. One of the regular diagrams for $K^+\to\pi^+\gamma_Y$ decay. Hyperphoton can be emitted by any of the quarks. Thus, three additional diagrams should also be considered.

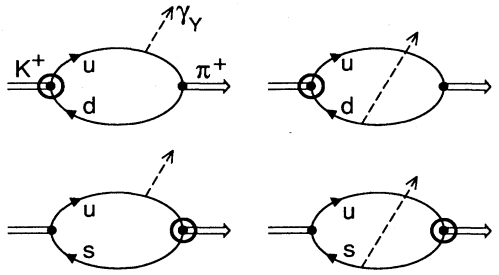

FIG. 11. The four diagrams with anomalous vertices.

and

$$J^\tau(1)=\left[k+\frac{P}{2}\right]^2\mathrm{Tr}\left[\gamma^\tau \not{P}\left[\not{k}+\frac{\not{P}}{2}\right]\not{R}\right]=J^\tau(3)\ ,$$
$$J^\tau(2)=\left[k-\frac{P}{2}\right]^2\mathrm{Tr}\left[\gamma^\tau \not{R}\left[\not{k}+\frac{\not{P}}{2}\right]\not{P}\right]\ , \tag{25}$$
$$J^\tau(4)=\left[k-\frac{P}{2}+Q\right]^2\mathrm{Tr}\left[\gamma^\tau \not{R}\left[\not{k}+\frac{\not{P}}{2}\right]\not{P}\right]\ .$$

When all the traces are calculated, and the loop integrals evaluated, the relevant part of the "anomalous" amplitude in model A, with $n=5$, becomes

$$A^\tau_{\rm anom}=-i\frac{G_F sc}{\sqrt{2}}ff_\pi f_K(4.7116Y^A_{(5)})P^\tau+\cdots\ . \tag{26}$$

In a similar way $A^\tau_{\rm anom}$ can be calculated in model B (for the result see the Appendix). It is important to note that the amplitude (26) is proportional to the parameter Y from the anomalous vertex (4), and not to X which played a role in the $K\to\pi\pi$ decays. This is the place where the assumption $X\approx Y$ [discussed after Eq. (21)] enters. If one uses $Y^A_{(5)}=1.3$ [compare to Eq. (21)], it becomes clear that the anomalous amplitude (26) completely dominates over the regular one, Eq. (22). Consequently, $K^+\to\pi^+\gamma_Y$ is another process in which regular diagrams could be totally neglected: diagrams with $s\to d$ transitions contain all the important physics. (A similar conclusion follows also in model B.) When the absolute square of the amplitude is multiplied by the appropriate phase-space factor, and divided by the total width, one finds the branching ratio B. For model A, this becomes

$$B=26.7(Y^A_{(5)})^2\frac{f^2}{m_Y^2}\times 10^{16}\ \text{eV}^2\ . \tag{27}$$

Here, m_Y is the mass of the hyperphoton. In Table III, parameters Y^A and Y^B are replaced by their numerical values, and the branching ratios are expressed in terms of the unknown quantity $(f/m_Y)^2$.

From the theoretical viewpoint, it is significant that the model A and model B results are so different, although both models gave the identical description of $K\to\pi\pi$. Clearly, the choice of wave functions plays the major role in a study of rare decays, and this is true not only for our diagrammatic approach, but also, as seen from Table III,

for all previous analyses. The big spread of the results basically reflects our inability to deal with long-distance physics. An optimistic view, that if we can correctly describe the main K-decay modes it automatically means we can trust the method in rare decays, is not at all supported by the above study.[34] Fortunately, in our example the physical consequences are unaffected. Even the lowest branching ratio in Table III seems to be excluded by experiments. Indeed, an upper limit on the strength of the fifth force can be deduced from the table, and one finds

$$\frac{f^2}{m_Y^2} \leq 9.2\times 10^{-24}\ \mathrm{eV}^{-2} = 60 G_\infty m_{\mathrm{H}}^2\ \mathrm{m}^2\ , \qquad (28)$$

where G_∞ is the gravitational constant, and m_{H} is the hydrogen mass. The upper bound (28) is not in agreement with findings from geophysical and other experiments. Therefore, it was suggested[35] that the fifth force might be coupled not exclusively to the hypercharge, but rather to a combination of hypercharge, strangeness, and isospin. Then a window for a superlight, vector carrier of the fifth force is still open.

As a final remark, let me repeat that the results in models A and B were obtained with the assumption that $Y \approx X$. With this assumption, the results more or less fit into the broad region charted by the other studies of the process. However, if by some reason it comes out that $Y \ll X$, the picture changes completely. In that case, the branching ratio for $K \to \pi\gamma_Y$ process becomes very small, and possibly even dominated by *regular* diagrams. As a consequence, even the pure hypercharge coupling of the fifth force could be saved. The option $Y \ll X$ should be considered seriously. Our limited knowledge of meson wave functions does not allow an *a priori* rejection of this possibility.

VI. CONCLUDING REMARKS

This work studies the long-standing problem of K decays from a new angle. Avoiding the short-distance expansion, it sets a scheme in which all QCD effects are absorbed in nonlocal effective vertices. The so-called "regular" vertex functions were introduced in a previous work,[8] and were found to describe surprisingly well *leptonic* and *semileptonic* K and π decays. In the present paper a further step is taken: an analytic form for a new kind of "anomalous" vertices is suggested. By combining regular and anomalous vertices, a quantitative description of *nonleptonic* K decays, and a simple parametrization of $\Delta I = \frac{1}{2}$ dominance, become possible.

It is also demonstrated that in a long-distance environment one *cannot* directly relate rare decays to the well-measured main decay modes of K. This fact was not apparent in analyses based on the operator expansions, because the leading short-distance corrections were preserving $(1\pm\gamma_5)$ chiral structure of operators. However, there is no reason to believe that the chiral structure will remain so simple when the long-distance QCD is taken into account. On the contrary, one would expect the structure to change to $(X + Y\gamma_5)$, with $|X|$ and $|Y|$ becoming unequal. X could be determined in $K \to \pi\pi$ decays, but not Y. Therefore, only a combination of rare decay amplitudes in which Y dependence cancels, will be related to the main two-body decay amplitudes.

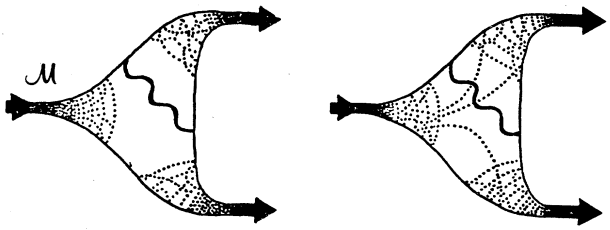

FIG. 12. Two-body weak decay of a meson. Dots indicate gluonic corrections. The corrections in the left diagram are included in the effective vertices.

Some elements of the proposed scheme still have to be improved or better understood. For example, it would be extremely helpful to have a theory which would shed some light on the form and parameters of the probability distributions and wave functions. Furthermore, although some QCD corrections are contained in the effective vertices, not *all* corrections are accounted for in the scheme. Consider, e.g., Fig. 12. The left diagram is properly treated by the model, but not the right diagram. Presently, it is very difficult to say anything about the importance of the diagrams from the latter subgroup. Closely related are problems caused by consideration of only the lowest Fock states in wave functions of mesons. It is easy to see that this limitation jeopardizes the gauge invariance of the theory.[10] To enable a study of radiative K and π decays, one should expand the model so that it also includes higher states, as represented, e.g., by $\mathcal{M}(q\bar{q}')\gamma$ vertices.

Although a need for further improvements cannot be denied, already in its present form the model provides a fresh look at some interesting aspects of K physics. For example, the precise form of the wave functions seems to be much more important in analyses of rare decays than previously thought. Long-distance physics and $s \to d$ transitions could be joined in a simple scheme characterized by a direct evaluation of full amplitudes. With only a few parameters, a fair description of all main decay modes of light mesons could be achieved, etc. Almost every physical problem can be approached from various starting points. Such a diversification is particularly needed in the study of K decays, where many important features are still not under control. The proposed new scheme might provide a path toward a more complete understanding of the old problem.

ACKNOWLEDGMENTS

It would have been impossible to complete this work without the support, encouragement, and criticism of many friends, particularly J. Eeg, E. Fischbach, B. Guberina, I. Picek, M. Scadron, and D. Tadić. I also want to thank R. Blankenbecler for the kind hospitality in the SLAC Theory Group. This work was supported by the Department of Energy, Contract No. DE-AC03-76SF00515.

APPENDIX: ALTERNATIVE MODEL FOR ANOMALOUS VERTICES

I am repeating here all the calculations mentioned in the main text in an alternative model. The goal of that study is to learn something about model dependency. In the alternative model ("model B"), the probability distribution for anomalous vertices has the form [compare to Eq. (4)]

$$\tilde{H}^{B}_{\mathcal{M}}(k,P)=\frac{1}{\pi^3}\frac{G_F sc}{\sqrt{2}}\beta_{\mathcal{M}}M_{\mathcal{M}}^{2n-3}\left[k\mp\frac{P}{2}\right]^2\frac{\not{P}(X^B+Y^B\gamma_5)}{(k^2-\alpha_{\mathcal{M}}P^2)^n}\ . \tag{A1}$$

Note that the power in the denominator is n, instead of $n+1$ used in model A. Expressions (5) and (8) remain unchanged, and so do the rules for evaluation of diagrams. Although the difference might look minor, the values of loop integrals change considerably in some cases.

Consider first the anomalous part of the $\pi^+\to\bar{l}\nu$ amplitude (Fig. 7). Instead of the expression in the second line of Eq. (11), one finds

$$(-)^n icf_\pi P^\mu\left[\frac{G_F s^2}{\sqrt{2}}M_\pi^2(X^B+Y^B)\frac{\alpha_\pi}{\pi^3}\left[\frac{1}{4\alpha_\pi}-\frac{2}{n-3}\right]\right]\ . \tag{A2}$$

Equation (13), for the amplitude $\tilde{A}(1)$ in $K_S\to\pi^+\pi^-$ decay, becomes replaced by

$$\tilde{A}(1)=\frac{G_F sc}{\sqrt{2}}\frac{1}{\pi^3}(\beta_K M_K^{2n-3})(\beta_\pi M_\pi^{2n-3})^2(-3)i^3\int\frac{d^4k}{(2\pi)^4}\frac{1}{\sqrt{2}}\left[\left[k+\frac{P}{2}\right]^2-\left[k-\frac{P}{2}\right]^2\right]$$
$$\times\mathrm{Tr}\left[\left[\not{k}+\frac{\not{P}}{2}-m_d\right]\frac{\not{P}(X^B+Y^B\gamma_5)}{B^n}\left[\not{k}-\frac{\not{P}}{2}-m_d\right]\frac{\not{S}\gamma_5}{C^n}\left[\not{k}+\frac{\not{S}-\not{R}}{2}-m_u\right]\frac{\not{R}\gamma_5}{D^n}\right]\ . \tag{A3}$$

The remaining two amplitudes, Eq. (19), get changed in a similar way, leading to the total anomalous amplitude [compare to Eq. (20)]

$$(\tilde{A}^{S}_{+-})_{\text{model B}}=\frac{G_F sc}{\sqrt{2}}M_K^2 f_\pi X^B\tilde{I}^B\ . \tag{A4}$$

With $n=5$, one finds $\tilde{I}^B\to\tilde{I}^B_{(5)}=-0.97$. Therefore, in order to describe the experimental value $\tilde{A}^S_{+-}\sim 376$ eV, one must choose $\tilde{X}^B_{(5)}\simeq -6.8$.

When the decay $K^+\to\pi^+\gamma_Y$ is considered, one finds that the amplitude A_{anom} becomes [compare to Eq. (23)]

$$A^\tau_{\text{anom}}=\frac{G_F sc}{\sqrt{2}}(\beta_K M_K^{2n-3})(\beta_\pi M_\pi^{2n-3})fY^B(-3)\int\frac{d^4k}{(2\pi)^4}\frac{1}{\pi^3}\left[\frac{C_u J^\tau(1)-C_d J^\tau(2)+C_u J^\tau(3)-C_s J^\tau(4)}{V^n U^n}\right]\ . \tag{A5}$$

This expression gives (with $n=5$)

$$(A^\tau_{\text{anom}})_{\text{model B}}=+i\frac{G_F sc}{\sqrt{2}}ff_\pi f_K(0.2114Y^B_{(5)})P^\tau+\cdots \tag{A6}$$

and the branching ratio

$$B=0.0537(Y^B_{(5)})^2\frac{f^2}{m_Y^2}\times 10^{16}\ \text{eV}^2\ . \tag{A7}$$

Whenever masses of quarks were required in calculations, in both models A and B, the values

$$m_u=m_d=0.010\ \text{GeV},\quad m_s=0.150\ \text{GeV}\ , \tag{A8}$$

were used. The other numerical constants, $G_F=1.1664\times10^{-23}\ \text{eV}^{-2}$, $s=0.222$, $c=0.975$, $M_K=0.495$ GeV, and $M_\pi=0.140$ GeV, have the standard values (see e.g., the Particle Data Group compilation[36]).

[1] S. Oneda, J. C. Pati, and B. Sakita, Phys. Rev. **119**, 482 (1960).

[2] M. Gell-Mann, in *Proceedings of the 1958 Annual International Conference on High Energy Physics at CERN*, edited by B. Ferretti (CERN, Geneva, 1958), p. 261.

[3] Many aspects of the K physics were thoroughly covered in *Hadronic Matrix Elements and Weak Decays*, proceedings of the Ringberg Workshop, Ringberg Castle, West Germany, 1988, edited by A. J. Buras, J.-M. Gérard, and W. Huber [Nucl. Phys. B (Proc. Suppl.) **7A** (1989)].

[4] See also the recent reivew, H.-Y. Cheng, Int. J. Mod. Phys. A **4**, 495 (1989).

[5] M. A. Shifman, A. I. Vainshtein, and V. I. Zakharov, Nucl. Phys. **B120**, 316 (1977).

[6] C. Bernard, T. Draper, G. Hockney, A. M. Rushton, and A.

Soni, Phys. Rev. Lett. **55**, 2770 (1985).
[7]C. Bernard, A. El-Khadra, and A. Soni, in *Hadronic Matrix Elements and Weak Decays* (Ref. 3).
[8]H. Galić, Z. Phys. C **29**, 519 (1985).
[9]H. Galić, Report No. SLAC-PUB-4788, 1988 (unpublished).
[10]H. Galić, Fizika **17**, 501 (1985).
[11]H. Galić, Phys. Rev. D **31**, 2363 (1985).
[12]P. Pascual and R. Tarrach, Phys. Lett. **87B**, 64 (1979).
[13]C. J. Gilmour, Z. Phys. C **18**, 163 (1983).
[14]S. P. Chia, Phys. Lett. **130B**, 315 (1983).
[15]E. P. Shabalin, ITEP Moscow Report No. 86-112, 1986 (unpublished).
[16]For $n=5$, the model gives, e.g., $I=0.67$. See Ref. 9 for a discussion.
[17]E. Fischbach, D. Sudarsky, A. Szafer, C. Talmadge, and S. H. Aronson, Phys. Rev. Lett. **56**, 3 (1986); **56**, 1427(E) (1986).
[18]S. C. Holding, F. D. Stacey, and G. J. Tuck, Phys. Rev. D **33**, 3487 (1986).
[19]A. T. Hsui, Science **237**, 881 (1987).
[20]P. E. Boynton, D. Crosby, P. Ekstrom, and A. Szumilo, Phys. Rev. Lett. **59**, 1385 (1987).
[21]D. H. Eckhardt, C. Jekeli, A. R. Lazarewicz, A. J. Romaides, and R. W. Sands, Phys. Rev. Lett. **60**, 2567 (1988).
[22]See also the recent review article by E. Fischbach and C. Talmadge, in *Fifth Force and Neutrino Physics* (proceedings of the XXIIIrd Rencontre de Moriond, VIIIth Moriond Workshop), Les Arcs, France, 1988, edited by O. Fackler and J. Tran Thanh Van (Editions Frontières, Gif-sur-Yvette, 1988), p. 369.
[23]It must be mentioned also that in several experiments no physically significant deviation was observed. For a list of these experiments, see, e.g., Ref. 22.
[24]F. D. Stacey *et al.*, Rev. Mod. Phys. **59**, 157 (1987).
[25]C. Talmadge and E. Fischbach, in *Proceedings of the International School of Cosmology and Gravitation,* Erice, Italy, 1987, edited by V. De Sabbata (Reidel, Dordrecht, in press).
[26]C. Talmadge and E. Fischbach, in *Fifth Force and Neutrino Physics* (Ref. 22), p. 413.
[27]E. Fischbach, D. Sudarsky, A. Szafer, C. Talmadge, and S. H. Aronson, Ann. Phys. (N.Y.) **182**, 1 (1988).
[28]Y. Asano *et al.* Phys. Lett. **107B**, 159 (1981); **113B**, 195 (1982).
[29]T. F. Kycia, spokesperson, BNL Experiment No. 787.
[30]M. Suzuki, Phys. Rev. Lett. **56**, 1339 (1986).
[31]S. H. Aronson, H.-Y. Cheng, E. Fischbach, and W. Haxton, Phys. Rev. Lett. **56**, 1342 (1986); **56**, 2334(E) (1986).
[32]C. Bouchiat and J. Iliopoulos, Phys. Lett. **169B**, 447 (1986).
[33]M. Lusignoli and A. Pugliese, Phys. Lett. B **171**, 468 (1986).
[34]Recently, another decay channel, namely, $K^0 \to \pi^+ \pi^- \gamma_Y$, was studied by J. Trampetić *et al.*, Phys. Rev. D **40**, 1716 (1989). Authors found that the analysis of this mode was much less dependent on details of calculation than in the mode $K^+ \to \pi^+ \gamma_Y$.
[35]See, e.g., S. Aronson, E. Fischbach, D. Sudarsky, and C. Talmadge, in *Fifth Force and Neutrino Physics* (Ref. 22), p. 593.
[36]Particle Data Group, G. P. Yost *et al.*, Phys. Lett. B **204**, 1 (1988).